

# Front-end Electronics Test for the LHCb Muon Wire Chambers

V. Bocci<sup>a</sup>, G. Carboni<sup>b</sup>, A. Massafferri<sup>b</sup>, R. Nobrega<sup>a</sup>, E. Santovetti<sup>b</sup>

<sup>a</sup> INFN Roma1 “La Sapienza”, Roma, Italy

<sup>b</sup> INFN Roma2 “Tor Vergata”, Roma, Italy

[rafael.nobrega@roma1.infn.it](mailto:rafael.nobrega@roma1.infn.it)

## Abstract

This document describes the apparatus and procedures implemented to test Multi Wire Proportional Chambers (MWPC) after front-end assembly for the LHCb Muon Detector. Results of measurements of key noise parameters are also described. Given a fully equipped chamber, this system is able to diagnose every channel performing an analysis of front-end output drivers' response and noise rate versus threshold. Besides, it allows to assess if the noise rate at the experiment threshold region is within appropriate limits. Aiming at an automatic, fast and user-friendly system for mass production tests of MWPC, the project has foreseen as well electronic identification of every chamber and front-end board, and data archiving in such a way to make it available to the Experiment Control System (ECS) while in operation.

## I. INTRODUCTION

### A. Chamber Readout Overview

The LHCb Muon System [1] is made of 19 geometrically different MWPC types. Depending on the chamber, the input capacitance as seen by the front-end electronics (FE) can vary from roughly 40pF to 250pF. Signals are collected from either anode or cathode; therefore a dedicated 8-channels Amplifier, Shaper and Discriminator (ASD) rad-hard chip, named CARIOCA [2], has been developed to process both polarities by means of two different pre-amplifiers in the ASD input stage. They show slightly different signal responses depending on the chosen polarity of operation. The on-detector circuitry is composed generally of two boards: Spark-Protection (SPB) and CARDIAC. The former board makes use of passive components while the latter processes and digitalizes chamber signals. A front-end card accommodates two CARIOCAs and a chip named DIALOG, [3] which has been developed to readout and control the CARIOCA chip. One DIALOG has one DAC per channel to control thresholds, 16 24-bit internal counters and features for timing adjustments of signals. An LHCb Muon specific software suite [4] was developed to study the behaviour of equipped chambers providing fully access to FEB features.

The main features of CARIOCA are:

- Sensitivity: 8-16 mV/fC
- Equivalent Noise Charge: 0.3-2 fC
  - 2240+42 e-/pF negative amplifier
  - 1880+45 e-/pF positive amplifier
- Offset:  $795.6 \pm 9.9$  mV ( $-35 \pm 5.5$  mV)
- Residual bias:  $35 \pm 5.5$  mV
- Max. Rate: 10-25 MHz (depending on polarity)

A 9.9 mV RMS offset can generate a large error while setting thresholds, as a consequence one separate threshold per channel can be set. A CARIOCA discriminator makes use of a Differential Threshold Voltage (DTV) circuit (1 per channel). It is able to provide a differential threshold from a reference voltage with single polarity. Apart from the offset spread there is a cut on the threshold range which does not allow setting values below a minimum (see Figure 1). This parameter has a charge value varying in the 2-4 fC range, depending on the input capacitance (for single input capacitance values measurements yield a RMS of 0.4 fC). Such a value can also be evaluated in terms of residual bias (discriminator characteristic). Theoretically this value is not correlated to the input capacitance and has a value of about  $\text{ResBias} = 35 \pm 5.5$  mV.

The noise (in Volts) and the threshold cut value can be directly measured by a threshold scan procedure as described in the next section. The threshold cut and the residual bias values can then be utilized in order to find the offset value of an ASD channel (the value at which the threshold is equivalent to zero Coulomb).

### B. Front-end Electronics Noise

Considering a charge sensitive amplifier, noise affects amplitude measurement resolution and, consequently, the minimum detectable charge value. Due to noise, the amplifier response has a certain statistical distribution. The probability density function describing the amplifier response in the presence of Gaussian noise can be expressed by:

$$f(V) = \frac{1}{\sqrt{2\pi}\sigma_n} e^{-\frac{V^2}{2\sigma_n^2}} \quad (1)$$

Given a discriminator threshold  $V_{th}$ , the probability that a sample results to be higher than such a threshold is given by:

$$P = \int_{V_{th}}^{\infty} \frac{1}{\sqrt{2\pi}\sigma_n} e^{-\frac{V^2}{2\sigma_n^2}} dV \quad (2)$$

The noise voltage ( $V_n$  as seen at the discriminator input), can be obtained from the sigma value of the function (2).

Theoretically a white noise process contains all frequency components with uniform amplitude. In practice, given some noise occurrence in a system, if its power level does not vary with frequency over the system operating range, the noise can be treated as a “white noise” process. Because power spectrum characteristics of this noise process are well known,

evaluating the response of a circuit it is possible to reconstruct the characteristics of its own bandwidth behaviour.

Considering a Gaussian noise presence in a discriminator input, and not taking into account bandwidth limitation, one can expect a threshold to noise ratio as represented by equation (3). Such an equation corresponds to the noise rate exceeding threshold level; with a signal baseline equal to  $V_{offset}$ .

$$f(V) = f_n \int_{V_{th}}^{\infty} e^{-\frac{1}{2} \frac{(V-V_{offset})^2}{V_n^2}} dV \quad \text{for } V_{th} \geq V_{offset} \quad (3)$$

where  $V_{th}$  is the threshold,  $V_n$  provides the noise in Volts and  $f_n$  is the sum of amplitude occurrences up to the mean value of the noise Gaussian amplitude.

Considering a Gaussian time distribution, the noise rate as a function of threshold can be approximately represented as follows:

$$f(V_{th}) = f_{n0} e^{-\frac{1}{2} \frac{(V_{th}-V_{offset})^2}{V_n^2}} \quad f_{n0} = \sqrt{\frac{1}{3} \frac{f_2^3 - f_1^3}{f_2 - f_1}} \quad (4)$$

Using formula (4) [5,6], the maximum noise rate  $f_{n0}$  (vertex frequency) can be calculated in terms of cutoff frequencies bandwidth parameters. Hence the vertex frequency can provide information about FE circuit bandwidth.

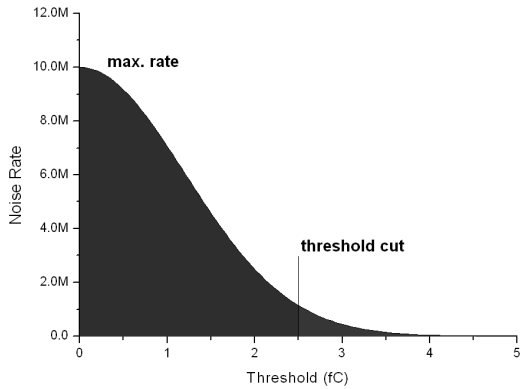


Figure 1 - Threshold scan for an offset equal to zero and considering bandwidth circuit characteristics.

It is possible to achieve a more precise value of  $V_n$  if it is considered noise rates below a certain frequency value, where the circuit bandwidth begins to affect the circuit response, and computing each of those measured noise rate values as follows:  $R_i = R_i - R_{i-1}$  (with  $V_{th(i)} > V_{th(i-1)}$ ). Using this procedure,  $V_n$  can be obtained from formula (1) parameters.

Since, it is only possible to make measurements above the threshold cut value (Figure 1, top); the formula below is used because it has been shown to be an efficient method to fit the noise curve. Figure 2 shows an example of the noise measurement method applied to analysis.

$$f(x) = e^{A-Bx} \quad x = V_{th}^2 \quad (5)$$

$$V_n = \sqrt{\frac{1}{2B}}$$

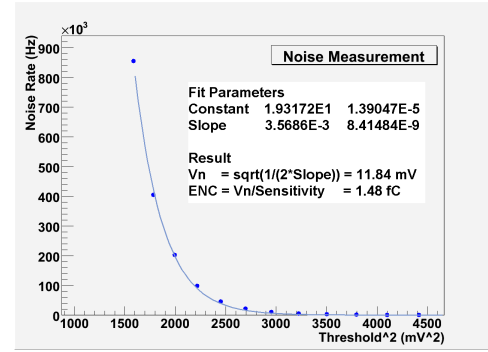


Figure 2 - Example of the noise curve measurement method.

By means of a threshold scan it is possible to obtain information about 2 important parameters of the circuit located before the discriminator: bandwidth and noise. An analysis as described above has been implemented in order to evaluate the method efficiency and has been utilized as a diagnostic tool for LHCb Muon Chamber Readout Electronics.

### C. Cdet Measurement

The front-end input capacitance (Cdet) is a fundamental parameter in the chamber readout test. A threshold scan procedure permits a direct measurement of noise in Volts and, as a result, an estimation of capacitance at the FE inputs (Cdet) through a direct conversion using a calibration curve (Figure 4). Fits of the known characteristics sensitivity and ENC curve of the ASD chip have been plotted (Figure 3), in order to use them analyzing the parameters of each CARIOCA, and to obtain the noise voltage value at the discriminator input for a given external threshold.

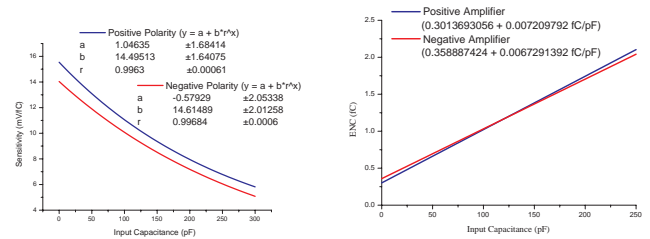


Figure 3 - CARIOCA sensitivity and noise curve (fit).

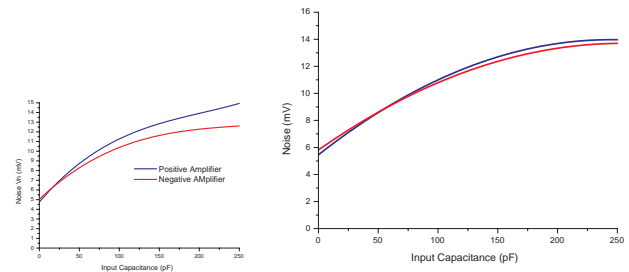


Figure 4 - CARIOCA noise at the discriminator input using the known sensitivity and noise curves (left) and directly measured.

The calibration curve (Figure 4 left side) obtained from sensitivity and noise characteristic curves are slightly different from the results of our measurements of noise voltage at the discriminator inputs. The calibration curve (Figure 4 right side) based on those measurements is used for the tests shown below.

## II. TESTING SETUP

The test setup consists of a MWPC equipped with front-end boards (DUT's), a barcode reader and control and readout circuitry, all supervised by a PC.

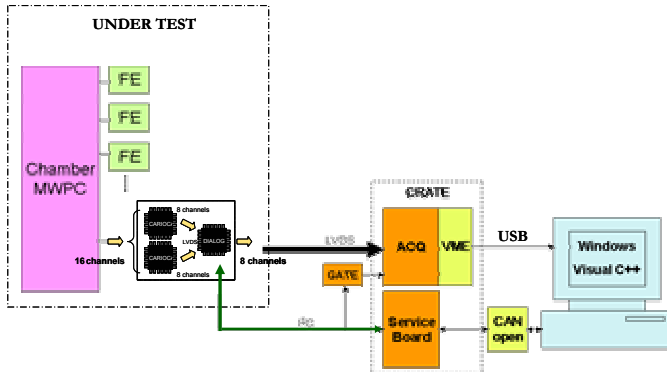


Figure 5 - Testing setup scheme.

### A. Control Equipment

Control is performed by means of a Service Board [7]. It can access in parallel all FEBs belonging to a chamber, generating pulses to be used mainly to inject signals and to control internal and external counters. This board is accessed using the CANopen protocol. To do so a commercial adapter manufactured by Kvaser Company has been used.

### B. Readout Electronics

There are 2 ways to readout the FEBs: by means of DIALOG internal counters or using the 64-channels counting module ACQ [8]. A gating board has been designed and used in order to translate the SB gate signal sent to the front-end into a pattern compatible with ACQ logic.

### C. Barcode Reader

During the chamber assembly, a ROOT (CERN analysis software) based program is used to identify and archive barcodes of chambers and their front-end boards. Afterwards, the Faraday cage (metal enclosure) is put into place, therefore not consenting direct access to the FEBs and their barcodes. The barcode information related to each FEB will be used later by analysis programs to access the database created as a result of FEB's production tests.

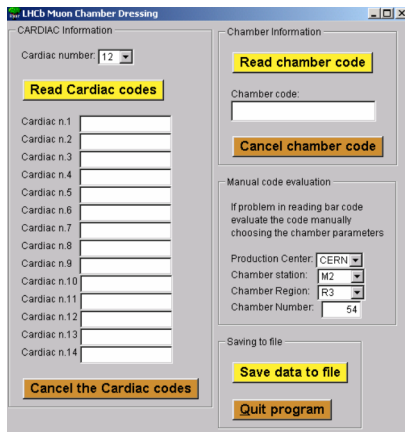


Figure 6 - Barcode reader program.

## D. Software

A Visual C++-ROOT integrated software tool has been developed to control all circuits, performing a diagnostic analysis of chambers and visualization of results.

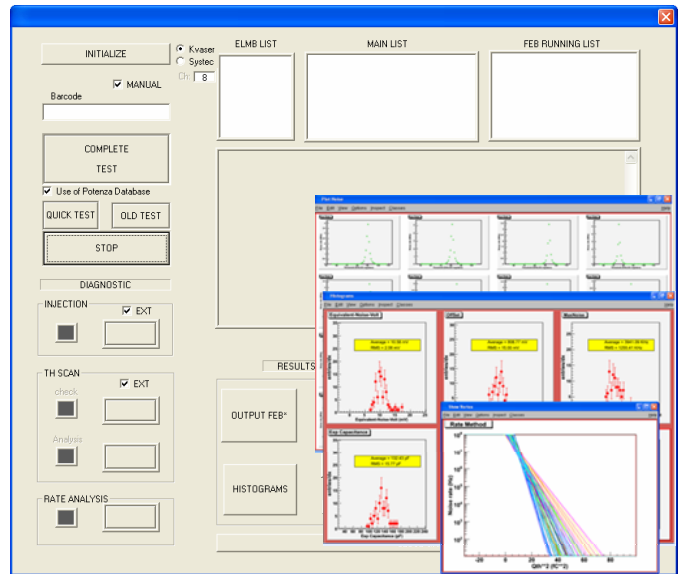


Figure 7 - Control, analysis and diagnostics software.

## III. PROCEDURES AND DIAGNOSTICS

### A. Cable checking and Auto-Injection

Once all the control and readout cables are connected, by means of injecting signals into the FEBs in a known sequence it can be verified that the cables are not inverted or there are false contacts.

Another procedure, checking if all FE channels respond to auto-injected generated signals, allows validating functionalities such as: auto-injection, internal counters and output drivers' response, making a comparison with the content of ACQ counters.

### B. Threshold Scan

With a threshold scan, a curve of threshold versus noise rate is generated, as shown in Figure 8. The threshold is in a range encompassing both polarities and, as shown before, it is performed in a range outside  $\pm 35$  mV.

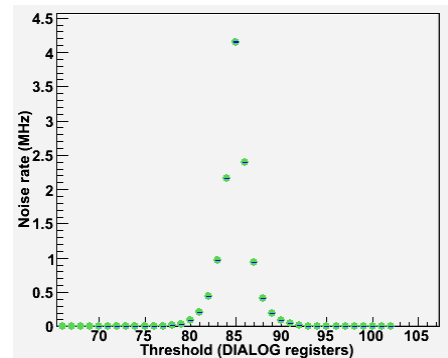


Figure 8 - Threshold scan curve.  $Th(mV) = Th(plot) * 2.42 + 625$

### 1) Noise presence and offset

A first analysis is carried out checking if the number of measured points obtained during the threshold scan is sufficient in order to fit the data. This is a useful tool to single out dead channels: if no points at all are found, the channel is marked as dead.

The offset value corresponds to the threshold value with the maximum rate of noise (from now on the term offset is used to indicate actually the value related to the threshold cut). Finally, the procedure verifies if the offset value found is within the limits given by the ASD characteristics (acceptance window), see Figure 9.

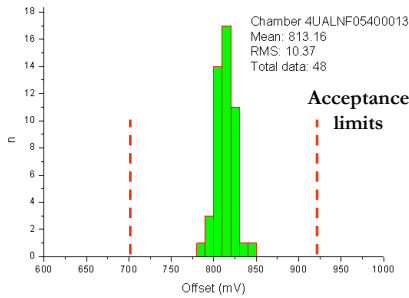


Figure 9 – Offset distribution example for the boards on an M5R4.

### 2) Noise rate versus threshold

After a fit of experimental data made using (5), the noise voltage ( $V_n$ ) parameter is calculated. Using the calibration curve (Figure 4) this value is converted directly into an estimate of detector capacitance. Then, the calculated capacitance values for all channels are averaged and the mean value should be within  $3 \cdot \text{RMS}$  from the nominal capacitance for the specific type of chamber under test.

The diagnostic routine subsequently verifies if Cdet of every channel is inside a 3 rms window (see Figure 10). If one or more channels are out of range, an alarm is raised; abnormal values are printed specifying their source.

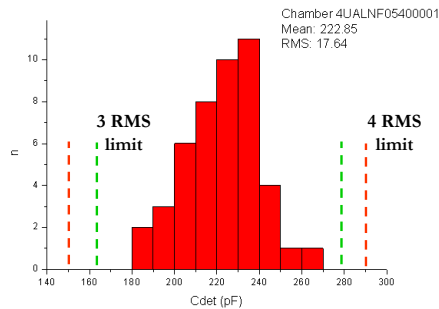


Figure 10 – Example of an estimated channel Cdet distribution for an M5R4 chamber.

### 3) Offset pattern recognition

From the threshold scan, a sequence of offset values can be obtained for the 16 channels of each FEB. This pattern is compared with the results obtained in the front-end mass production test, in order to check if the FEBs on the chamber have been correctly identified. Measurement data is archived to be used later; such data can be also utilized to identify chambers during their assemblage on the wall.

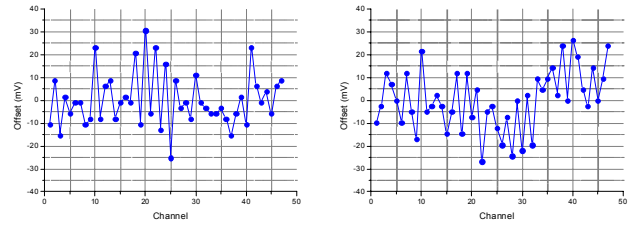


Figure 11 –Pattern (subtracting the average) of 2 M5R4 chambers.

### C. Noise rate at the nominal threshold region

The LHCb Muon TDR [1] requires a maximum noise rate of 100Hz per channel for MWPCs. Recent studies of LHCb Muon Detector have shown that channels with a noise rate up to a few kHz are not critical.

The diagnostic tool is able to measure the electronics noise rate at different thresholds (in the vicinity of the nominal value). If the noise rate measured at  $(\text{Thnom} + \Delta)$  is higher than 1 KHz, an error condition is signalled.

## IV. ESTIMATION OF CDET MEASUREMENT ERROR

The error of Cdet measurement has been estimated considering single channels tested at 4 different known capacitances (56, 100, 180 and 220 pF) with about 90 measurements per capacitance value (4 16-channels capacitor boards were built in order to perform such tests). The results showed that it is possible to measure a channel input capacitance with a precision better than 7 pF if all channels had been calibrated before executing tests; however, this is impractical due to the huge number of channels to test.

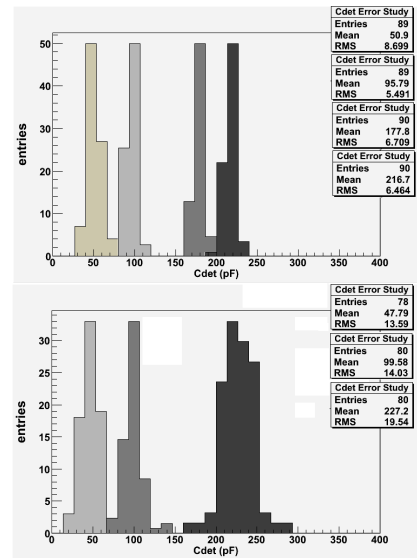


Figure 12 - Error measurement for a calibration curve per channel and per a group of channels.

When evaluating different channels of a group of boards the system becomes less accurate due to the spread on FE channels characteristics. The error found in this case was estimated to be 20 pF; Figure 12 shows measurement of 5 different FEBs with capacitances of 47, 100 and 220 pF. The accuracy of the measurements presented is satisfactory to evaluate chamber capacitance and single channels.

## V. RESULTS

About 120 MWPCs from INFN production sites (Ferrara, Firenze and Frascati) have been tested to date; the results are presented here. During the tests, chambers with out of acceptable range values have been repaired. Therefore, all parameters shown in the measurements below are within specification.

### A. M5R4 Frascati

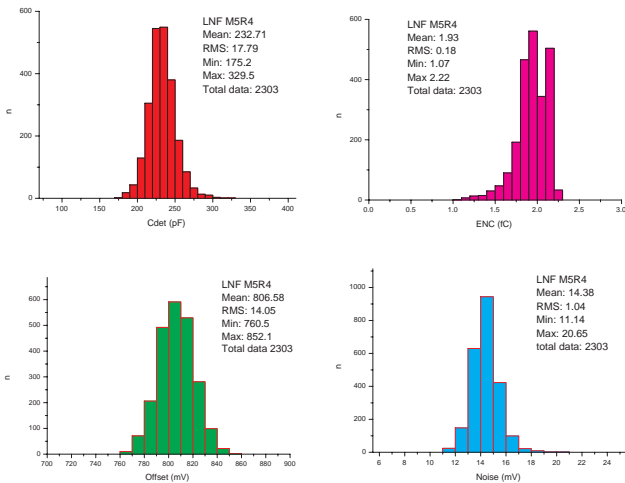


Figure 13 - Results for the LNF M5R4 chambers.

### B. M5R3 Frascati

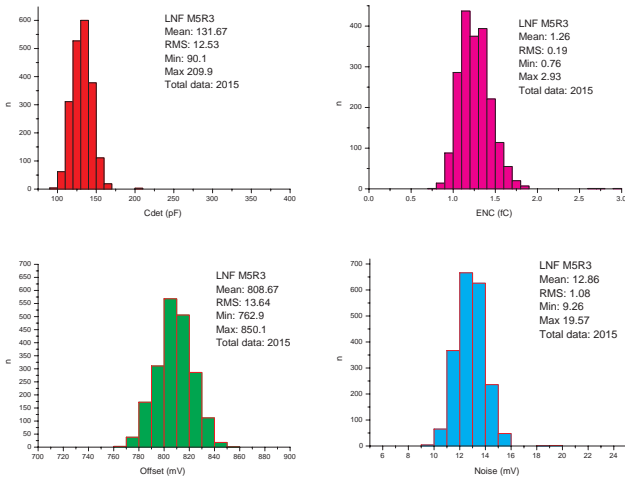


Figure 14 - Results for the LNF M5R3 chambers.

### C. M5R4 Firenze

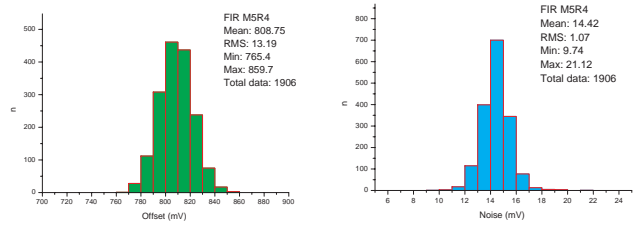
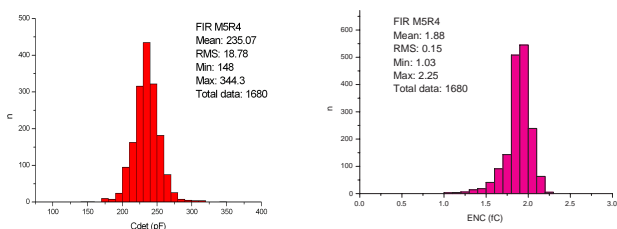


Figure 15 - Results for the Firenze M5R4 chambers.

### D. M5R2 Ferrara

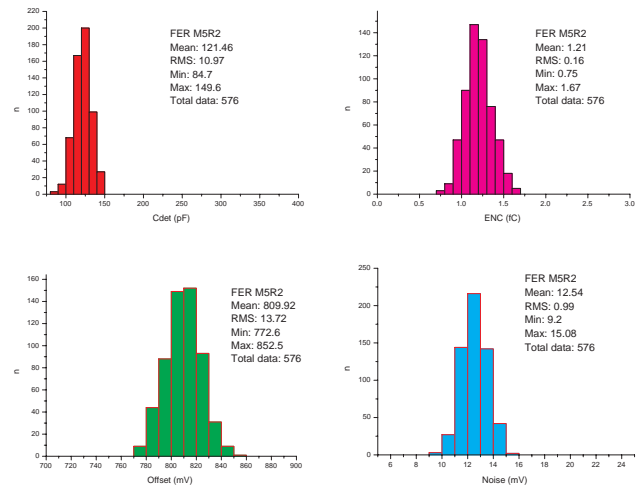


Figure 16 - Results for the Ferrara M5R2 chambers.

## VI. CONCLUSION

The goal of this project was to implement an automatic and fast system (accessible also to non experts) for the mass production tests of LHCb Muon MWPCs. Chambers that do not pass the tests must be the object of remedial action. By means of using the diagnostic method presented, we aim at reducing to a minimum the number of chambers to undergo more time consuming test.

## VII. REFERENCES

- [1] LHCb Collaboration, "LHCb Muon System TDR", CERN/LHCC 2001-010 (2001) and "Addendum to the Muon System TDR", CERN/LHCC 2003-002 (2003).
- [2] N.Pelloux, "Architecture&Layout Overview", June 2003.
- [3] S.Cadeddu, et al, Nuclear Instruments and Methods in Physics Research A 518 (2004), 486.
- [4] R.Nobrega, "Software tool to Debug the LHCb Muon Chambers Front-End Electronics", LHCb-2006-042.
- [5] see for instance: H.Spieler, "Rate of Noise Hits in Threshold Discriminator Systems", (1998). Lecture Notes, Physics 198, Spring Semester 1998, UC Berkeley.
- [6] A.Kashchuk, LHCb Muon Technical Note 2002-013.
- [7] V.Bocci et al, "Service Board – Datasheet", INFN sezione Roma, Italy, 2003.
- [8] A.Balla et al, "ACQ Manual", INFN LNF, Italy, 2003.